# Spin-density-wave behaviour of the $(Cr_{100-x}Al_x)_{95}Mo_5$ alloy system

**B Muchono, A R E Prinsloo, C J Sheppard, H L Alberts and A M Strydom**

Physics Department, University of Johannesburg, P.O. Box 524, Auckland Park, Johannesburg 2006, South Africa

E-mail address: alettap@uj.ac.za

**Abstract.** Electrical resistivity, Seebeck coefficient and specific heat measurements on a $(Cr_{100-x}Al_x)_{95}Mo_5$, $0 \leq x \leq 8.1$ at.% Al alloy system are reported. The results indicate two possible quantum critical points in the magnetic phase diagram of this system. One is an incommensurate spin-density-wave – paramagnetic quantum critical point situated at $x \approx 1.5$ at.% Al and the other a paramagnetic – commensurate spin-density-wave critical point at $x \approx 5$ at.% Al. We forward experimental evidence that this system harbours two spin-density-wave related quantum critical points which presents an unusually rich case study for magnetic quantum criticality of the itinerant kind.

## 1. Introduction

Cr and its dilute alloys are exceptional examples of spin-density-wave (SDW) type itinerant electron antiferromagnetic (AFM) systems. The $Cr_{100-x}Al_x$ alloy system is of particular interest. It presents both incommensurate (I) and commensurate (C) SDW AFM phases, as well as a paramagnetic (PM) phase in its magnetic phase diagram. There exists a triple point at $x_c \approx 2$ at.% Al, where these three phases coexist [1]. Previous studies [2] comprising electrical resistivity and magneto-elastic measurements on alloys of $Cr_{100-x}Al_x$ with Mo in ternary $(Cr_{100-x}Al_x)_{95}Mo_5$ suggest that SDW AFM is suppressed down to at least 4 K in the concentration range $2.0 \leq x \leq 5.0$ at.% Al. The current interest in quantum criticality of Cr and its dilute alloys [3, 4] therefore warrants further detailed investigations on the $(Cr_{100-x}Al_x)_{95}Mo_5$ system, particularly on critical effects and the possibility of having simultaneously two types of SDW QC points (QCP's) in the same Cr alloy system. Here we report results of the temperature dependence of the electrical resistivity as well as of the Seebeck and Sommerfeld coefficients of thermoelectricity and specific heat, respectively, for a more comprehensive range of alloys in the concentration range $0 \leq x \leq 8.1$ at.% Al.

## 2. Experimental

Ternary $(Cr_{100-x}Al_x)_{95}Mo_5$ alloys were prepared by arc melting in a purified argon atmosphere from 99.999 at.% pure Cr, 99.999 at.% pure Al and 99.99 at.% pure Mo. The alloys were annealed in an ultra-high pure argon atmosphere at 1300 K for three days and quenched in iced water. The actual elemental composition and homogeneity were checked by electron microprobe analyses. Electrical resistivity ($\rho$), Seebeck coefficient ($S$) and specific heat ($C_p$) were measured in the range $2 \leq T \leq 350$ K, using standard Quantum Design PPMS equipment incorporating appropriate measuring options [5].

## 3. Results and discussion

Figure 1 shows three typical examples of $\rho(T)$ curves, one each for the CSDW, PM and ISDW alloys in the $(Cr_{100-x}Al_x)_{95}Mo_5$ system. For ISDW alloys ($x \lesssim 1.5$ at.% Al), $\rho(T)$ depicts a well defined anomaly in the form of a minimum near the Néel transition temperature ($T_N$), figure 1(a), which is typically also observed in other ISDW Cr alloys [1]. This is attributed to an induced SDW energy band gap at the Fermi energy upon cooling through $T_N$ [1]. The $\rho(T)$ anomaly is absent for alloys in the concentration range between 1.5 and 5.3 at.% Al, indicating that alloys in this concentration range remain PM down to 2 K, as indicated in figure 1(b). The reappearance of AFM, accompanied by a $\rho(T)$ magnetic anomaly of CSDW origin is conspicuous in figure 1(c) for $x \gtrsim 5$ at.% Al [1, 2]. The $\rho(T)$ anomaly in the CSDW phase is however much weaker than that in the ISDW phase, contrary to expectations for CSDW Cr alloys [1].
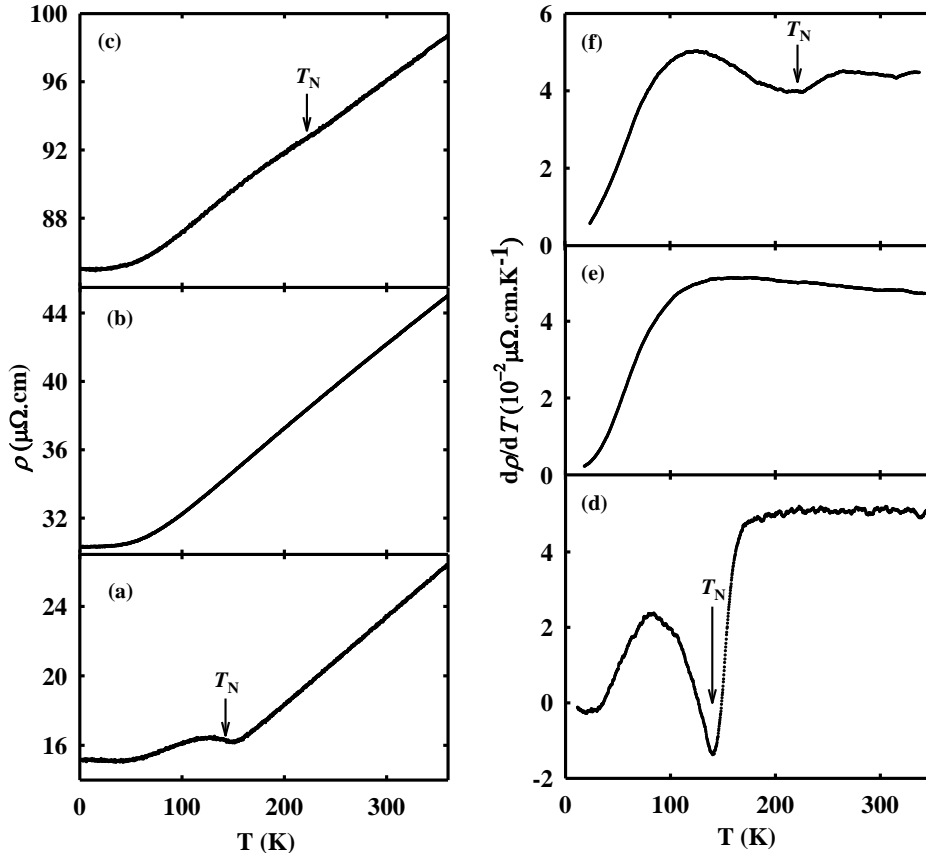


**Figure 1**: Typical examples of the temperature dependence of the electrical resistivity, $\rho(T)$, and its temperature derivative $(d\rho(T)/dT)$ of the $(Cr_{100-x}Al_x)_{95}Mo_5$ alloy system. Shown are an ISDW alloy with $x = 1.0$ [(a) and (d)], a PM alloy with $x = 2.8$ [(b) and (e)] and a CSDW alloy with $x = 6.1$ [(c) and (f)] at.% Al. The Néel temperature ($T_N$), shown by arrows, is obtained from the $d\rho(T)/dT$ minimum. The experimental error in the absolute value of $\rho$ amounts to $\approx 5\%$ and originates mainly from errors in determining the sample dimensions, while changes in $\rho$ of 0.5% or better could be detected as a function of temperature.

$T_N$ is often defined for Cr and its dilute alloys as the temperature of the minimum in $d\rho(T)/dT$ accompanying the $\rho(T)$ magnetic anomaly [1] and this definition is appropriately also used for the present $(Cr_{100-x}Al_x)_{95}Mo_5$ system. Figures 1(d), (e) and (f) depict the temperature dependence of $d\rho(T)/dT$, obtained from figures 1(a), (b) and (c), respectively, with the position of $T_N$ marked by an arrow. The SDW anomaly is clearly better defined in $d\rho(T)/dT$ than in $\rho(T)$ itself. $T_N$ values thus obtained are plotted on the magnetic phase diagram displayed in figure 4(a).

It may be mentioned that $T_N$ is in some instances obtained for Cr and its alloys by back extrapolation of the $\rho(T)$ curves, from temperatures high up in the PM phase down to 0 K [6]. This generates a PM base-line curve, should the alloy remains PM down to 0 K, from which the magnetic component, $\Delta\rho(T)$, of $\rho(T)$ can be extracted. $T_N$ is then taken at the temperature where $\Delta\rho(T)$ tends to zero. This was tested on the ISDW $x = 1.0$ at.% Al alloy, giving results that compare to within 10 K with that obtained from $d\rho(T)/dT$. Applying this method to the CSDW alloys is however problematic, as the present measurements do not extend to high enough temperatures above $T_N$ for a reliable back extrapolation.

Seebeck coefficient, $S(T)$, measurements are useful and complementary [1] to $\rho(T)$ measurements for obtaining $T_N$ of Cr alloys, particularly for those alloys showing weak SDW $\rho(T)$ anomalies near $T_N$. The reason is the fact that the carrier diffusion component of $S(T)$ depends on the energy derivative of the electrical conductivity at the Fermi energy, resulting in a much stronger $S(T)$ anomaly on SDW formation than that for $\rho(T)$ [1]. $S(T)$ measurements on the $(Cr_{100-x}Al_x)_{95}Mo_5$ alloys are therefore also reported here. Figure 2(a), (b) and (c) show typical examples for ISDW, PM and CSDW alloys, indicating the higher sensitivity of $S(T)$ for the Néel transition.
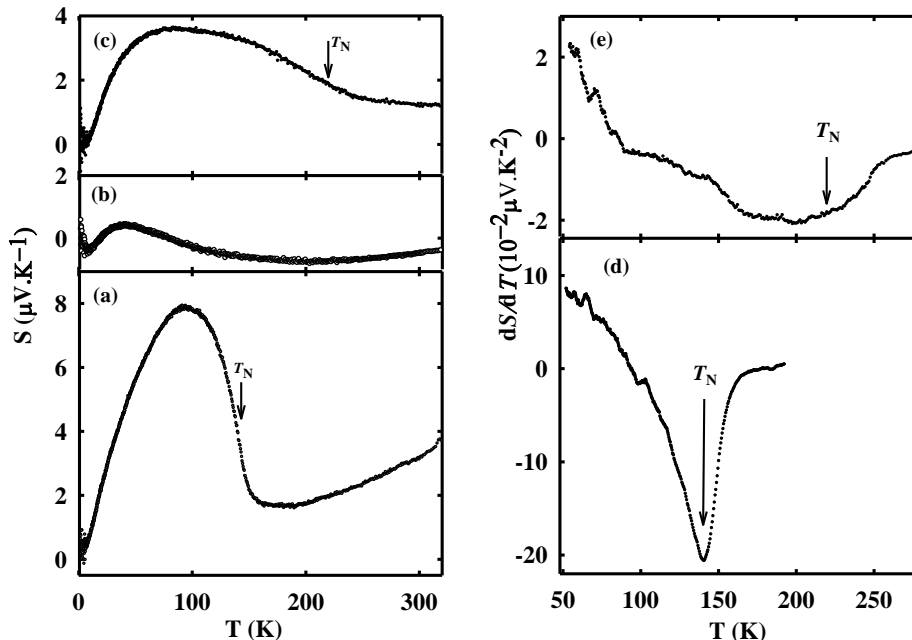


**Figure 2**: The temperature dependence of Seebeck coefficient ($S$) and its temperature derivative ($dS(T)/dT$) of the $(Cr_{100-x}Al_x)_{95}Mo_5$ alloy system. Shown are an ISDW alloy with $x = 1.0$ [(a) and (d)], a PM alloy with $x = 2.8$ (b) and a CSDW alloy with $x = 6.1$ [(c) and (e)] at.% Al. The Néel temperature ($T_N$), shown by the arrows, is taken at the minimum point of $d\rho(T)/dT$. The standard deviation in the measurement of the thermal voltage in the calculation of $S (= dV/dT)$ is typically less than 0.5%.

$T_N$ values obtained from $d\rho(T)/dT$ are indicated by arrows in these figures. $dS(T)/dT$ curves for the two AFM alloys of figures 2(a) and (c) are shown in figure 2(d) and (e), respectively, together with $T_N$ obtained from $d\rho(T)/dT$. There is reasonably good correspondence between values of $T_N$ obtained from the temperature derivatives of $\rho(T)$ and $S(T)$ respectively, which provides confidence in our method for obtaining $T_N$.

Figure 3 shows three typical examples, one each for ISDW, CSDW and PM alloys, of low temperature $C_P/T$ vs. $T^2$ plots obtained from $C_P(T)$ measurements on the $(Cr_{100-x}Al_x)_{95}Mo_5$ alloys in the temperature range $2 \le T \le 60$ K. The curves are fitted rather well by the low-temperature approximation of the Debye formulation of specific heat, $C_p(T) = \gamma T + \beta T^3$, where $\gamma$ represents the Sommerfeld electronic specific heat coefficient and the last term is representative of the lattice specific heat contribution. $\gamma(x)$, obtained from linear $C_P/T$ vs. $T^2$ plots for the various alloys are shown in figure 4(b). The curve shows interesting behaviour that is related to influences of effects of SDW formation on the electronic density of states at the Fermi energy and spin fluctuation effects.
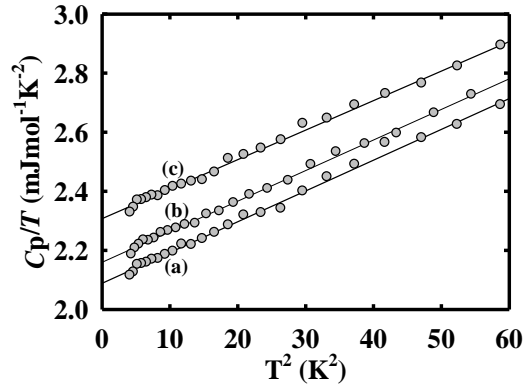


**Figure 3**: Graphs of $C_P(T)/T$ vs. $T^2$ plotted for three typical $(Cr_{100-x}Al_x)_{95}Mo_5$ alloy examples at low temperatures: (a) an ISDW alloy with $x = 1.0$, (b) a CSDW alloy with $x = 6.1$ and (c) a PM alloy with $x = 2.8$ at.% Al. The solid lines through the data points represent least-square linear fits. The experimental error in $C_P(T)/T$ is about 1%.
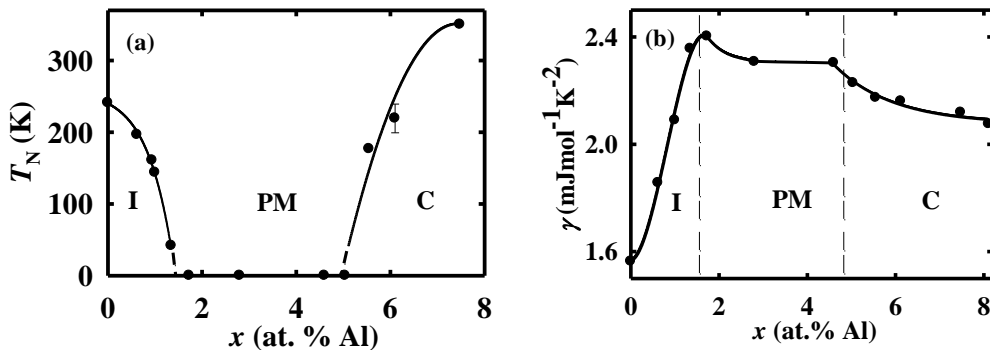


**Figure 4**: (a) The magnetic phase diagram and (b) the Sommerfeld coefficient, $\gamma$, as a function of Al concentration, $x$, for the $(Cr_{100-x}Al_x)_{95}Mo_5$ alloy system. I, PM and C denotes incommensurate spin-density-wave, paramagnetic and commensurate spin-density-wave phases, respectively. The experimental error in $T_N$ is shown by an error bar while the experimental error in $\gamma$ is within the size of the experimental points. The solid lines are guides to the eye.

Of interest is the sharp rise of $\gamma(x)$ in the ISDW phase that is followed by a slow decrease, becoming nearly flat, in the PM phase and eventually decreases relatively sharply on entering the CSDW phase. This behaviour is understood by considerations of Takeuchi's [7] application of Hasegawa's [8] spin fluctuation theory for $\gamma$ of itinerant electron antiferromagnetic systems, to the case of $Cr_{100-y}V_y$ alloys. This alloy system depicts [4] an ISDW-P QCP on the magnetic phase diagram at $y_c = 3.4$ at.% V, a point up to which $\gamma(y)$ increases sharply, followed by a rather slow decrease in the PM phase [7]. It was shown that the slow decrease of $\gamma(y)$ in the PM phase, $y > y_c$, of this system is well explained by spin fluctuation effects alone, while the sharp decrease at $y < y_c$ resulted from a combination of SF and ISDW energy gap influences, the latter outweighing that of spin-fluctuations [7]. Following this reasoning one then expects $\gamma(x)$ of the $(Cr_{100-x}Al_x)_{95}Mo_5$ system also to follow this trend on increasing $x$ through the two QCP's: a sharp rise up to a peak at the ISDW-P QCP, followed by a rather slower decrease in the PM phase, and the possibility of a second small peak, before $\gamma(x)$ decreases again on entering the CSDW phase through the P-CSDW QCP, as shown in figure 4(b). $\gamma(x)$, which is related to the electronic density of states at the Fermi energy, thus appears to be an excellent parameter for indications of QC behaviour in this alloy system.

## 4. Conclusion

The present study substantially expands and corroborates earlier studies on the magnetic phase diagram of $(Cr_{100-x}Al_x)_{95}Mo_5$. The results, particular the behaviour of the concentration dependence of the Sommerfeld electronic specific heat coefficient, are in evidence of the presence of two quantum critical points on the magnetic phase diagram of the $(Cr_{100-x}Al_x)_{95}Mo_5$ alloy system. It is then rather exceptional to observe both ISDW-P and P-CSDW quantum critical points in the same Cr alloy system. Hall coefficient and magnetic susceptibility are critical parameters [3, 4, 9] for exploring quantum criticality in Cr and its alloys and further investigations in this regard as well as exploring the possibility of a second peak in $\gamma(x)$ (figure 4 (b)) are underway for the present $(Cr_{100-x}Al_x)_{95}Mo_5$ alloys.

**Reference list**
[1]   Fawcett E, Alberts H L, Galkin V Yu, Noakes D R and Yakhmi J V 1994 *Rev Mod. Phys.* **66** 25
[2]   Smit P and Alberts H L 1993 *J. Phys.: Condens. Matter* **5** 6433
[3]   Jaramillo A, Feng Y, Wang J, and Rosenbaum T F 2010 *Proc. Nat. Acad. of Sci.* USA **107** 16361
[4]   Yeh A, Soh Y, Brooke J, Aeppli G and Rosenbaum T F 2002 *Nature* **419** 459
[5]   Quantum Design, 6325 Lusk Boulevard, San Diego, CA 92121-3733, USA
[6]   Alberts H L, Prinsloo A R E and Strydom A M 2010 J. *Magn. Magn. Mater.* **322** 1092
[7]   Takeuchi J, Sasakura H and Masuda Y 1980 *J. Phys. Soc. Jpn.* **49** 508
[8]    Hasegawa H 1975 *J. Phys. Soc. Jpn.* **38** 107
[9]    Paschen S 2006 *Physica* B **378-380** 28